Fragmentation increases impact of wind disturbance on forest structure and carbon stocks in a western Amazonian landscape

Running head: Forest fragmentation and wind disturbance

Authors: Naomi B. Schwartz[1], María Uriarte[1], Ruth DeFries[1], Kristopher M. Bedka[2], Katia Fernandes[3,4], Victor Gutiérrez-Vélez[5], Miguel A. Pinedo-Vasquez[3,4]

1. Department of Ecology, Evolution, and Environmental Biology, Columbia University, New York, NY 10027 USA

2. NASA Langley Research Center, Hampton, VA 23681 USA

3. International Research Institute for Climate and Society, Columbia University, Palisades, NY 10964

4. Center for International Forestry Research, Bogor, Indonesia 16115

5. Department of Geography and Urban Studies, Temple University, Philadelphia, PA 19122.

Corresponding author: Naomi B. Schwartz, (212) 854-9987, nbs2127@columbia.edu

Keywords: tropical forest, second-growth forest, carbon, wind disturbance, forest fragmentation, remote sensing, Amazon

Paper type: primary research

Abstract

Tropical second-growth forests could help mitigate climate change, but the degree to which their carbon potential is achieved will depend on exposure to disturbance. Wind disturbance is common in tropical forests, shaping structure, composition, and function, and influencing successional trajectories. However, little is known about the impacts of extreme winds in fragmented landscapes, though second-growth forests are often located in mosaics of forest, pasture, cropland, and other land cover types. Though indirect evidence suggests that fragmentation increases risk of wind damage, few studies have found such impacts following severe storms. In this study, we ask whether fragmentation and forest type (old vs. second growth) were associated with variation in wind damage after a severe convective storm in a fragmented production landscape in western Amazonia. We applied linear spectral unmixing to Landsat 8 imagery from before and after the storm, and combined it with field observations of damage to map wind effects on forest structure and biomass (Figure 4, 5). We also used Landsat 8 imagery to map land cover with the goals of identifying old- and second-growth forest and characterizing fragmentation. We used these data to assess variation in wind disturbance across 95,596 hectares of forest, distributed over 6,110 patches. We find that fragmentation is significantly associated with wind damage, with damage severity higher at forest edges and in edgier, more isolated patches (Figure 7). Damage was more severe in old-growth than in second-growth forests, but this effect was weaker than that of fragmentation (Figure 8). These results illustrate the importance of considering spatial configuration and landscape context in planning tropical forest restoration and predicting carbon sequestration in second-growth forests. Future research should address the mechanisms

behind these results, to minimize wind damage risk in second-growth forests so their carbon potential can be maximally achieved.

Introduction

Tropical second-growth forests recover biomass quickly after clearing and can sequester large amounts of carbon (Poorter et al., 2016). These forests could play an important role in mitigating climate change; for example, if allowed to grow undisturbed, existing Latin American second-growth forests could accumulate an additional 8.48 Pg C in the next 40 years, enough to offset all carbon emissions from fossil fuel use and industrial processes in Latin America and the Caribbean from 1993-2014 (Chazdon et al., 2016). However, exposure to natural disturbances such as extreme winds, fires, or drought can affect successional trajectories in second-growth forests (Flynn et al., 2009; Anderson-Teixeira et al., 2013, Uriarte et al. 2009, Uriarte et al. in revision), influencing the degree to which the carbon sequestration potential of second-growth forests is achieved. Furthermore, second-growth forests, by definition, are located in landscapes subject to human influence that are mosaics of old growth, second growth, and other land cover types. Regrowth often happens along existing forest margins (Asner et al., 2009; Sloan et al., 2015), making second-growth forests highly exposed to edge effects, impacts of fragmentation, and anthropogenic disturbances. Accurately predicting biomass recovery in these forests requires that we understand their disturbance ecology and how their disturbance regimes are influenced by the landscapes in which they are situated.

Wind is a major disturbance in the tropics and has both short-term impacts and lasting legacies in tropical forests (Everham & Brokaw, 1996; Laurance & Curran, 2008; Lugo, 2008). Tropical forests are exposed to extreme winds from tropical storms or via convective downdrafts, squall lines and isolated cold fronts. Convective downdrafts and squall lines are relatively common in the Amazon basin (Garstang et al., 1994; 1998), and associated extreme winds can cause large-scale forest disturbance and tree mortality (Espírito-Santo *et al.*, 2010; Negrón-Juárez *et al.*, 2010). Tropical storms and heavy precipitation events are expected to become more intense with climate change (Knutson et al. 2010, Orlowsky and Senevirante, 2012), and warming and land use change will affect future convection patterns (Del Genio *et al.*, 2007; Ramos da Silva *et al.*, 2008). Understanding the determinants of forest susceptibility to extreme winds is thus important for modeling and monitoring future impacts of forest disturbance (US DOE, 2012).

The spatial distribution and size of blowdowns have important consequences for understanding biomass dynamics in tropical forests (Fisher *et al.*, 2008; Chambers *et al.*, 2009; Di Vittorio *et al.*, 2014). A number of studies have quantified the frequency, return interval, rotation period, and carbon impacts of large blowdowns in the Amazon across expanses of old-growth forest (Nelson *et al.*, 1994; Negrón-Juárez *et al.*, 2010; Chambers *et al.*, 2013; Espírito-Santo *et al.*, 2014). However, little is known about the impacts of extreme winds in the fragmented, mosaic landscapes in which tropical second-growth forests occur. If forest fragmentation increases the impacts of wind disturbance, this difference could affect estimates of potential carbon sequestration in tropical second-growth forest.

Studies examining impacts of extreme winds in second-growth forests have found differences due to species composition and forest structure. Damage is most severe for pioneer species, species with low wood density, taller trees, and trees with a larger diameter for a given height (Zimmerman *et al.*, 1994; Curran *et al.*, 2008; Canham *et al.*, 2010; Uriarte *et al.*, 2012; Rifai et al. 2016, Putz *et al.*, 1983; Everham & Brokaw, 1996;

McGroddy *et al.*, 2013). Stand structure characteristics such as canopy height, canopy density, basal area, and median diameter are positively correlated with the amount of wind damage in a stand (Everham & Brokaw, 1996; Uriarte *et al.*, 2004; McGroddy *et al.*, 2013). Susceptibility to damage increases with stand age in earlier stages of succession, but may decline in older stands (Everham & Brokaw, 1996). These shifts are due to both changes in forest structure and changes in species composition: though canopy height, density, and basal area increase over succession, species composition often shifts away from low wood-density pioneers towards late-successional species with harder wood (Bazzaz & Pickett, 1980; Lohbeck *et al*., 2013).

Though second-growth forests are often highly fragmented and located in mosaic landscapes, few studies have considered the influence of landscape and patch structure on wind damage. Fragmentation may influence exposure to strong winds because wind speeds vary with surface roughness, with winds gaining more speed over low-roughness vegetation such as open grassland, brush, or agricultural crops (Fons, 1940; Oliver, 1971; Davies-Colley *et al.*, 2000). Accordingly, wind speeds decline with distance from forest-pasture edges (Davies-Colley *et al.*, 2000), and there is strong wind turbulence at high-contrast forest edges (Somerville, 1980; Morse *et al.*, 2002). Wind also moves more quickly though open forest (Somerville, 1980; Kanowski *et al.*, 2008), and forest edges have lower biomass and a more open canopy (de Casaneve *et al.*, 1995; Laurance *et al.*, 1997b; Harper *et al.*, 2005). The risk of blowdowns may also be higher at forest edges because pioneer species are more common (Oosterhoorn & Kappelle, 2000; Laurance *et al.*, 2006).

Despite variation in exposure and vulnerability to extreme winds, evidence for impacts of fragmentation on wind damage in tropical forests is lacking. Though several studies in temperate silvicultural systems have detected edge effects on wind damage (Peltola, 1996; Talkkari *et al.*, 2000; Zeng *et al.*, 2004), this effect has been more challenging to detect in diverse tropical forests. The Biological Dynamics of Forest Fragments experiment in the Brazilian Amazon found high tree mortality close to forest edges, with uprooting more frequent relative to standing dead trees (Ferreira & Laurance, 1997; Laurance *et al.*, 1997a; Mesquita *et al.*, 1999). However, this mortality was not linked to specific extreme wind events and could have resulted from other factors (e.g., desiccation). A few studies have examined fragmentation effects on wind damage after tropical storms, and have found little evidence that damage varies with fragmentation (Catterall *et al.*, 2008; Grimbacher *et al.*, 2008). The degree to which fragmentation increases the risk of damage from extreme winds in tropical forests thus remains an open question.

Detecting effects of fragmentation on wind damage may be difficult with a field sampling approach. Extreme winds can be highly patchy (Bellingham *et al.*, 1992; Imbert *et al.*, 1996; Grove *et al.*, 2000; Pohlman *et al.*, 2008). Detecting spatial patterns within heterogeneous, patchy phenomena requires large sample sizes, and inadequate sampling can make it difficult or impossible to detect patterns (Loehle, 1991). Estimates of landscape level mortality based on field plot observations may miss up to 17% of mortality (Chambers *et al.*, 2013), and field plot studies may lack the statistical power to detect the effect of fragmentation on wind damage (Grimbacher *et al.*, 2008). However, remote sensing allows detection of patterns that may be unfeasible or impossible in ground-based studies (Chambers *et al.*, 2007). Recently developed remote sensing techniques can detect gaps as small as 0.1 ha (Negrón-Juárez *et al.*, 2011). Unlike plot-based approaches, remote sensing allows estimation of wind damage across broad areas, and in combination with field data can improve our understanding of disturbance and carbon dynamics in tropical mosaic landscapes.

Here, we use remotely sensed data to quantify damage from a mesoscale convective storm system across a fragmented production landscape in the Peruvian Amazon. We use these data in combination with maps of land cover to ask:

1) Are second-growth forests more severely fragmented than old-growth forests?
2) How does fragmentation influence forest vulnerability to extreme winds?
3) Does wind damage severity vary in old-growth versus second-growth forests?

We predict that second-growth forests in our study area will be more severely fragmented than old-growth forests, and hypothesize that severity of wind damage will be highest in small, isolated forest fragments and close to forest edges. We expect that second-growth forests, which have a higher proportion of soft-wooded pioneer species, will suffer more severe damage than old-growth forests, composed of less vulnerable hard-wooded species. This variability could affect forest succession in dynamic, fragmented landscapes, with forest patch and landscape characteristics influencing rates of biomass recovery via effects on exposure and vulnerability to wind disturbance.

Materials and methods

Study area

The city of Pucallpa, the capital of the Ucayali region of Peru, is the largest Amazonian city connected to the national capital, Lima, by road. As a result, Pucallpa is an important transport center, and in recent years has been a hotspot of forest disturbance, deforestation, and fire in the Peruvian Amazon (Oliveira *et al.*, 2007, Schwartz et al., 2015, Uriarte et al., 2012). This research focuses on an area of 2,158 km^2 near Pucallpa, surrounding the highway from Lima to Pucallpa. The landscape is heterogeneous, with patches of old growth and second-growth forest surrounded by pastures, oil palm plantations, and smallholder farms (Gutierrez-Velez et al., 2013; Figure 1). Elevation ranges from 150 to 250 m a.s.l. and total annual precipitation ranges from about 1500-2500 mm, with a dry season from July to September.

Figure 1: Location of the study area, near Pucallpa, Ucayali, Peru. Inset depicts forest cover, and locations of field plots and roads.

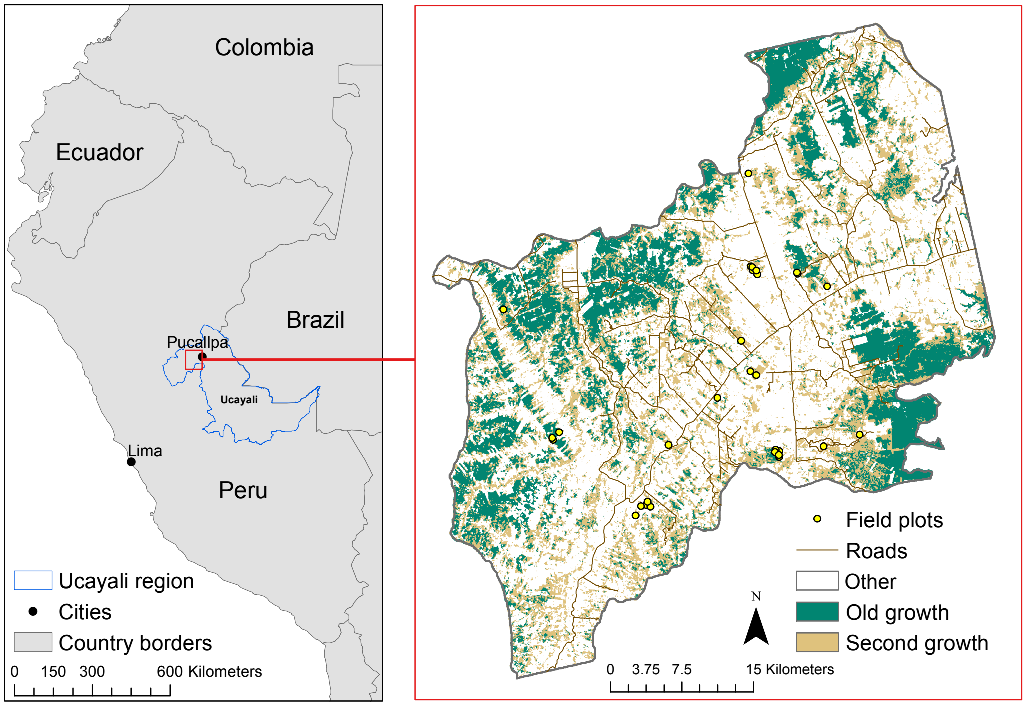

On November 30, 2013, a mesoscale convective system (MCS) passed through the study area, resulting in widespread blowdowns and tree mortality. Though there is insufficient meteorological station data available from the study area to characterize the storm severity, data processed from the GOES-13 satellite using the method described in Bedka and Khlopenkov (2016) indicates high overshooting top probability during the November 30 storm in the study area (Figure S1). Overshooting tops indicate regions where strong updrafts were present within the MCS. Strong downdrafts are often present near to these updrafts in regions of heavy precipitation. Storms with overshooting tops often generate winds that exceed 58 mph, the criterion for “damaging wind” by the U.S. NOAA National Weather Service (Dworak et al. 2012). Given the heterogeneity in land cover, forest age, and patch size, this landscape offers an ideal opportunity to study how impacts of damaging winds vary with fragmentation and landscape context.

Remote sensing of wind damage

We obtained Landsat 8 OLI scenes covering the study area (path-row 06-066 and 07-066) from 2013 (pre-storm) and 2014 (post-storm; Table S1) at 30 m resolution. All scenes were calibrated and converted to surface reflectance via the L8SR algorithm (http://landsat.usgs.gov/documents/provisional_l8sr_product_guide.pdf) and downloaded from the Landsat CDR archive via USGS Earth Explorer (http://earthexplorer.usgs.gov/). The Landsat OLI surface reflectance product includes a cloud mask created by the FMASK algorithm (Zhu & Woodcock, 2012), which we used to mask pixels that were cloudy in either 2013 and 2014. 1023 ha were masked out due to cloud cover, equal to 0.5% of the study area. Scenes were radiometrically normalized by applying the MAD algorithm (Canty & Nielsen, 2008). This procedure reduces differences across scenes from atmospheric effects not corrected by the L8SR algorithm. All remote sensing data processing was conducted in ENVI (Exelis Visual Information Solutions, Boulder, Colorado) unless otherwise indicated.

To map wind damage we follow the approach outlined by Negron-Juarez et al. (2010, 2011), which uses spectral mixture analysis (SMA) to map the change in non-photosynthetic vegetation (NPV) fraction across pixels. SMA assumes that every pixel is a linear combination of some number of target endmember spectra, such as vegetation, shade, NPV, and/or bare soil, and quantifies the per-pixel fraction of each endmember (Adams & Gillespie, 2006). Wind damage increases the amount of wood, dead vegetation, and litter exposed to the sensor, and so the change in NPV fraction is associated with the amount of wind damage. In a study in the Amazon, the signal lasted for about one year following an extreme wind event, until post-storm recovery generated sufficient new leaf biomass to obscure the NPV signal (Negrón-Juárez *et al.*, 2010).

We applied linear spectral unmixing to each image using endmembers for green vegetation (GV), NPV, and shade. Endmembers were identified from the reference scene using the Pixel Purity Index algorithm (Boardman *et al.*, 1995) available in ENVI (Figure S2). Following unmixing, we normalized the fraction of NPV without shade as NPV/(GV+NPV) so that fractions reflected only relative proportions of NPV and GV, and not differences due to effects of shading (Adams & Gillespie, 2006). Change in NPV (ΔNPV) was calculated by subtracting the normalized NPV fraction in 2013 from 2014.

Field data collection: Wind damage was measured in the field to assess whether ΔNPV provided an adequate approximation of damage. During the months of July and August of 2014 and 2015, we established 30-0.1 ha forest plots (Figure 1). We used satellite images to identify second-growth forest patches, and from those, chose sites where we could locate and get permission from the landowners. Within these areas, plot locations were selected to encompass a range of ΔNPV. Because plots were slightly larger than a Landsat pixel, plot-level ΔNPV was calculated as the weighted mean of ΔNPV in pixels overlapped by the plot. Plots were geolocated using a Garmin GPSMAP 62sc.

In each plot we measured diameter at breast height (dbh) of all trees greater than 5 cm, and coded each tree as damaged (uprooted, trunk snapped, or severe branch loss) or undamaged. Downed or damaged trees that were severely rotted were marked as such, since these trees were likely damaged prior to the 2013 storm. We conducted all analyses including and excluding these previously damaged individuals and it did not significantly affect our results; reported results exclude these trees. We calculated aboveground biomass (AGB) using the following allometric equation developed for second-growth forest in Panama (Van Breugel et al. 2011):

$$\ln(\text{biomass}) = -1.863 + 2.208*\text{DBH}$$

We divided biomass by two so that estimates were in terms of kg C instead of kg biomass, under the assumption that C makes up 50% of biomass (Brown and Lugo, 1982). To characterize plot-level damage, we calculated total damaged biomass, proportion biomass damaged, total stems damaged, and proportion of stems damaged for each plot. We assessed the accuracy of ΔNPV for mapping wind damage by calculating linear regressions of ΔNPV vs. field measurements of wind damage in the 30 forest plots. To estimate AGB loss across the study area, we used the parameters from the linear model of ΔNPV vs. total AGB lost.

Remote sensing of land cover: We developed a land cover classification at 30 m resolution for use in generating predictor variables related to fragmentation and masking analyses to forested areas. The classification expanded on the approach laid out in Gutierrez-Velez and DeFries (2013). Land use classes were old-growth forest, second-growth forest, mature oil palm (> 3 years old), and “other,” which included young oil palm (< 3 years old), bare ground, burned non-forest areas, fallow, pasture, degraded pasture, and bodies of water. Second-growth forests were defined as tree-dominated vegetation growing in areas that had previously been cleared. These areas have significantly lower basal area than old-growth forests in the study area (Gutiérrez-Vélez *et al.*, 2011). Old-growth forests are predominantly residual forest from logging and extraction of non-timber resources, but they have never been cleared and have significantly higher basal area and biomass than second-growth forests. For details on other land cover classes, see Gutierrez-Velez and DeFries (2013).

We classified Landsat 8 OLI images (Table S1) and with a random forest classification built with several spectral indices and spectral transformations: i) NDVI, ii) bare soil, vegetation, and shade fractions from SMA, iii) brightness, greenness, and third from a tasseled cap transformation, and iv) first- and second-order texture measures. Components i-iii were shown to be effective for classifying the non-oil palm land cover classes in a land cover classification from the same study area (Gutiérrez-Vélez & DeFries, 2013). Component iv, the texture measures, were useful for distinguishing oil palm plantations, which are spectrally similar to secondary forests but appear more uniform in satellite images due to even-aged planting. Training and testing data for land cover classes were collected during a 2015 field campaign and included 2198.52 ha total, divided among classes (Table S2). For more details about the classification, see Supporting Information.

The land cover map from 2014 was used to mask analyses to forested areas (old growth and second growth). We also masked areas near known anthropogenic disturbance, since spillover disturbance from recent forest clearing might bias results along forest edges. To do so, we identified recently deforested areas – areas that were classified as forest in 2013 and as non-forest in 2014 – and masked all pixels within 60 m to prevent anthropogenic disturbance biasing results (Figure S3).

Characterizing forest fragmentation: We used Fragstats (McGarigal et al. 2012) to characterize forest patch fragmentation. Old-growth and second-growth forests were all treated as a single forest category for the purpose of characterizing patches. Fragmentation has three key axes: area, edge, and isolation (Fahrig, 2003; Haddad *et al.*, 2015). We calculated one Fragstats metric to represent each of these axes (Figure 2). Patch area (ha) represents patch size. Edginess is quantified with the shape index, which is calculated as:

$$SHAPE = \frac{0.25p}{\sqrt{a}}$$

where p is the patch perimeter and a is the patch area. Shape index increases as the perimeter of a patch gets more complex, and equals 1 if a patch is a perfect square. We quantified isolation with the proximity index. The proximity index takes into account the area and distance of forest within a particular radius around the focal patch, and increases from zero with the upper limit determined by the search radius. For a given patch *I*, proximity index is calculated as:

$$PROX = \sum_{j=1}^{n} \frac{a_{ij}}{h_{ij}^2}$$

where a_{ij} is the area (m^2) of patches $j=1 \ldots n$ within specified neighborhood radius (m) of focal patch i and h_{ij} is the distance (m) between patch i and patch j. Using this formulation assumes that larger and closer patches decrease patch isolation more than smaller or more distant ones, a reasonable assumption. We calculated proximity index with several radii (250 m, 500 m, 1000 m, 2000 m, 4000 m and 10000 m), but these indices were highly correlated and there was no significant different in model performance depending on the distance, so we used the 1000 m radius in our final models. So that higher values represented increasing isolation, we multiplied proximity index by -1.

Figure 2: Conceptual figure illustrating axes of fragmentation, and variables associated with fragmentation included in analyses. Green squares represent forest pixels, and adjacent pixels represent a patch. Orange outline indicates focal pixel/patch for distance to edge and isolation measures.

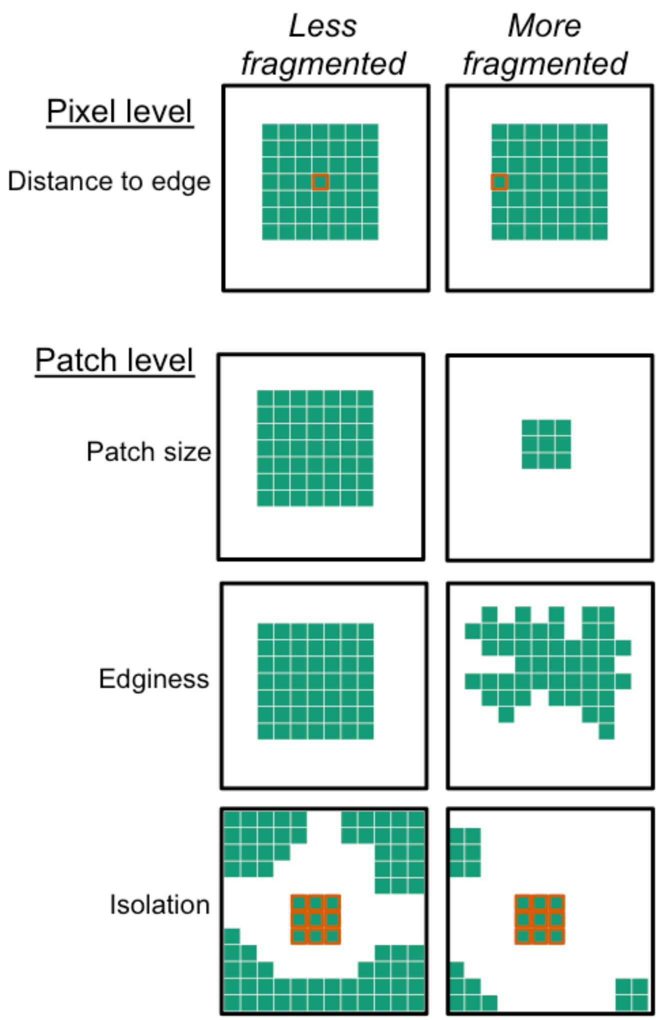

Statistical analysis: We compared sizes of damaged vs. undamaged trees, and fragmentation variables in old- vs. second-growth forest using t-tests. To test the relationship between wind damage, forest fragmentation, and forest age (old vs second growth), we fit a generalized linear model to predict ΔNPV at the pixel scale (Table 1). Pixels with ΔNPV less than 0 were excluded from analysis, because a decline in NPV cannot represent negative damage and instead likely represents changes due to forest succession or recovery from prior disturbance. Both pixel characteristics and patch characteristics were included as predictors. Pixel level predictors were distance from forest edge and a binary predictor for second-growth forest (0 = old growth, 1 = second growth). Patch level predictors were area, edginess, and isolation of the patches in which pixels were located. Because the total number of pixels was large (461,610) and ΔNPV was highly left skewed, we stratified pixels according to ΔNPV (0-0.05, 0.05-0.15, 0.15-0.25, >0.25) and randomly sampled 2000 pixels from each stratum for use in statistical analyses (Figure S4). The sample was bootstrapped 200 times. ΔNPV was log-transformed to meet the assumption of normality. Distance from edge was also log-transformed because it was highly left-skewed. To facilitate interpretation, all predictors were scaled to unit standard deviation by subtracting the mean and dividing by the standard deviation (Gelman and Hill, 2007). To test for collinearity among predictors we calculated variance inflation factors (VIF; Fox & Monette, 1992). VIF values greater than ~5 indicate strong collinearity (Dormann *et al.*, 2012). VIF for all predictors was < 4 with the exception of edginess (VIF = 5.2). To address this potential collinearity issue we ran the model with all predictors other than patch area, which was correlated with the other fragmentation predictors and was the predictor with the weakest effect in the full model. The maximum VIF in this partial model was 2.2, and the results for all remaining predictors were qualitatively the same as in the full model. Here, we present the full model, including area. We tested for spatial autocorrelation among model residuals by calculating Moran's I and found no spatial autocorrelation in the model residuals (Moran's I = 0.0003, p = 0.45). Model parameters reported are the median estimates of the 200 bootstrapped models and 95% bootstrapped confidence intervals. Statistical analyses were conducted in R (R Core Team, 2016).

Table 1: Model covariates, descriptions, and summary statistics.

Variable name	***Description***	***Landscape mean (SD)***	***Bootstrap sample mean (95% bootstrapped CI)***	***Bootstrap sample SD (95% bootstrapped CI)***
Response				
ΔNPV	Change in non-photosynthetic vegetation fraction in pixel, i.e. wind damage (log transformed).	0.034 (0.039)	0.1560 [0.1556, 0.1565]	0.1318 [0.1312, 0.1322]
Predictors				
Distance to edge	Pixel distance to forest edge (meters)	102.5 (2.5)	69.4 [68.0, 70.8]	2.39 [2.36, 2.44]
Secondary	Binary variable for second growth. 0 = old growth, 1 = second growth	0.53 (0.50)	0.59 [0.58, 0.60]	0.491 [0.490, 0.493]
Area	Patch size in which pixel is located (hectares).	33247.5 (28869.9)	33035.4 [32503.2, 33605.0]	30899.6 [30592.6, 31200.1]
Edginess (shape index)	Shape index for patch in which pixel is located.	24.4 (14.6)	24.9 [24.6, 25.2]	15.9 [15.7, 16.0]
Isolation (-1* proximity index)	Proximity index for patch in which pixel is located.	75887.7 (50523.7)	-71336.3 [-72230.3, -70415.9]	48734.9 [47999.9, 49327.5]

Results

Overview: linking field and remote sensing data

Validation of Δ NPV with field observations: Mean pre-damage AGB in field plots was 37.03 Mg C ha^{-1} (s.d. = 13.31). Mean AGB damaged was 9.76 Mg C ha^{-1} (s.d. = 10.49), or 23.4% of pre-storm AGB (s.d. = 24.4%). Mean stem density in field plots was 1286 stems ha^{-1} (s.d. = 342.6), with an average 16.5% of stems damaged (s.d. = 15.7). Damaged stems were significantly larger than undamaged stems (Figure 3, t = -9.73, $p < 0.0001$).

Figure 3: Frequency distributions and box plots of tree sizes for undamaged vs. damaged trees. Boxes show 25, 50, and 75% quantiles and whisker endpoints are 2.5 and 97.5% quantiles.

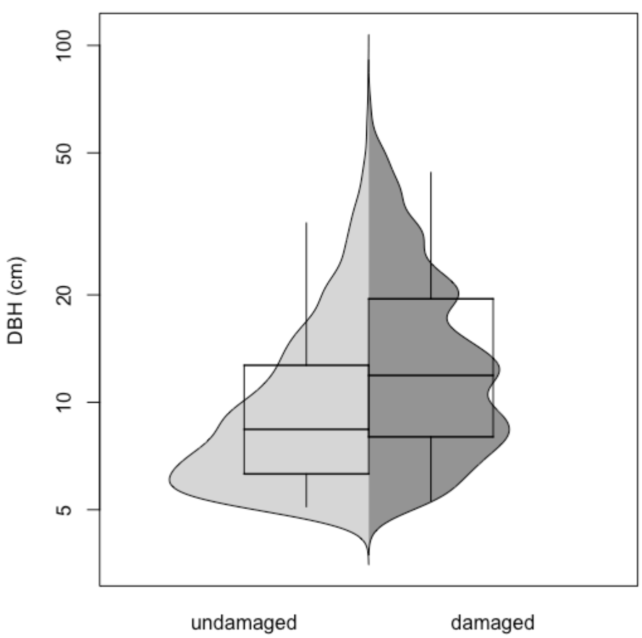

Δ NPV was strongly related to damage as measured in the field plots. It was most strongly correlated with the proportion of stems damaged in field plots (R^2 = 0.699, Figure 4), but the relationship held when damage was quantified in terms of total number of stems damaged (R^2 =0.649), total AGB damaged (R^2 = 0.574), or proportion of AGB damaged (R^2 = 0.603, Figure S5). On average ΔNPV was low across the landscape: mean ΔNPV was 0.03, and standard deviation was 0.04 (Figure 5). Five percent of forest pixels, or 2058 ha, had ΔNPV higher than 0.1, corresponding to 20.7% stems damaged, or 30.7% of AGB damaged (12.8 Mg C ha^{-1}). ΔNPV was greater than 0.2 in 0.8% of forest pixels (348.5 ha), corresponding to 48.6% stems damaged, or 78.5% of AGB lost (32.9 Mg C ha^{-1}). The total biomass lost as a result of the wind storm across the study area was approximately 1.68 Tg C.

Figure 4: ΔNPV vs. proportion of stems > 5 cm DBH damaged in field plots. Shaded areas indicate 95% confidence interval of regression line.

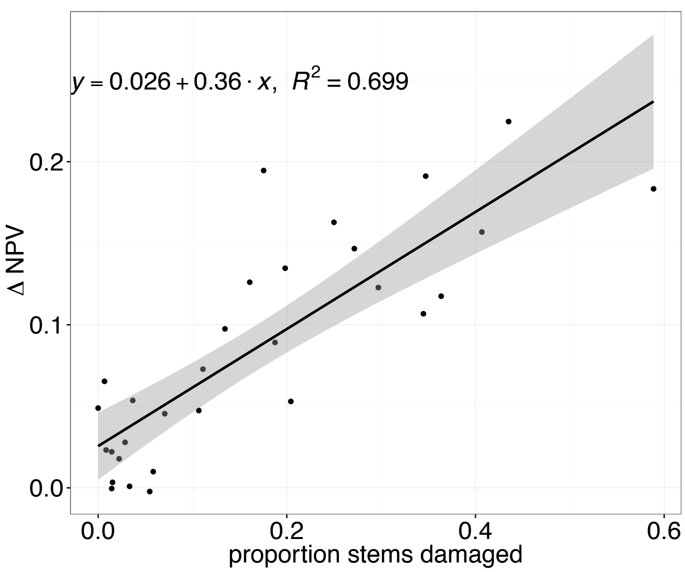

Figure 5: Map of wind damage (ΔNPV) in study area. Insets show two areas of interest where several field plots were located.

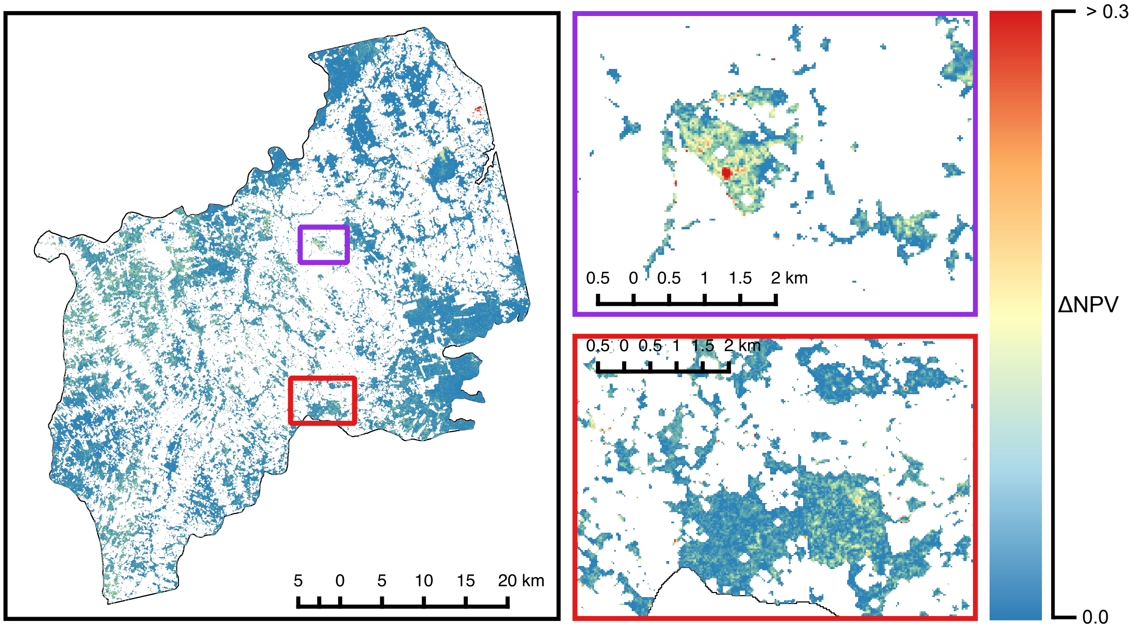

Characterizing land cover and fragmentation: The land cover classification accurately distinguished between oil palm, old-growth forest, second-growth forest, and other classes (Table S3). Overall accuracy was 96.4%. Forty-four percent of the study area, 95,596 ha, was classified as forest. Forty percent of forest pixels were classified as old-growth forest, and 60% were classified as second-growth forest (Figure 1). There were 6110 forest patches in the study area, with a mean area of 42.1 ha (Figure S6). Mean edginess (shape index) was 1.3, and mean isolation (-1*proximity index) was -19688 (Figure S6).

Fragmentation in old- vs. second-growth forests

Degree of fragmentation varied across old-growth and second-growth forest pixels, with second-growth forests more fragmented along most measures (Figure 6). Second-growth forest pixels were closer to forest edges ($t = 237.15$, $p < 0.001$), but in less edgy patches ($t = 134.76$, $p < 0.0001$). Second-growth pixels were also located in smaller ($t = 141.28$, $p < 0.001$, Figure 6) and more isolated patches, ($t = 47.658$, $p < 0.0001$, Figure 6).

Figure 6: Comparison of the distribution of fragmentation variables between old-growth and second-growth forest pixels. Boxes show 25, 50, and 75% quantiles and whisker endpoints are 2.5 and 97.5% quantiles of observed data. Light grey points are outliers. Figures include data from all forest pixels in the study area. Fragmentation variables are a) distance to edge, b) area, c) edginess, and d) isolation.

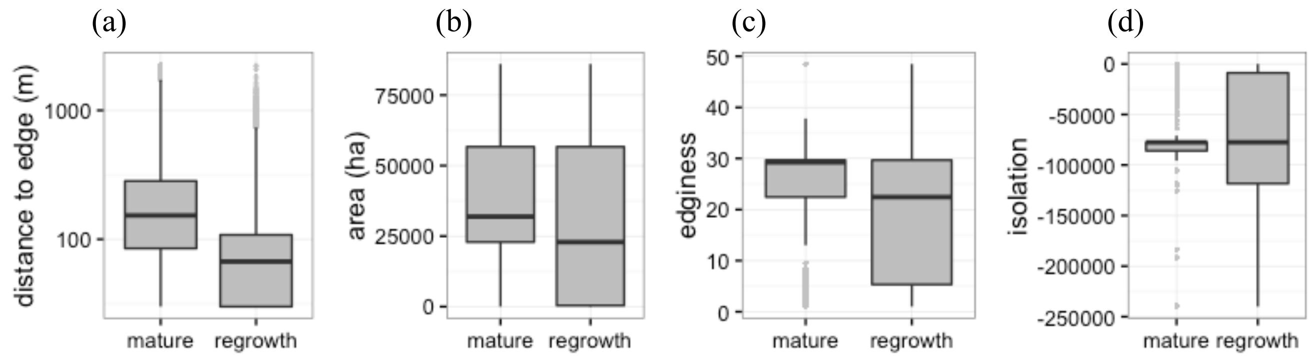

Wind damage model

Fragmentation and forest type were significantly associated with ΔNPV ($R^2 = 0.158$, 95% bootstrap CI = [0.143, 0.173]). Distance to edge had the strongest association with ΔNPV (Figure 7), which exponentially decreased with pixel distance from forest edge (Figure 8a). Patch edginess was positively associated with ΔNPV, with pixels in edgier patches suffering more severe wind damage (Figure 7, Figure 8c). Isolation also influenced damage: ΔNPV was higher in more isolated patches (Figure 7, Figure 8d). Patch area was negatively associated with damage, though this effect was weaker than that of the other fragmentation predictors (Figure 7, Figure 8b). Predicted ΔNPV was slightly higher for old-growth forest pixels, though the difference between second growth and old growth was small compared to the predicted variation in ΔNPV associated with fragmentation (Figure 7, Figure 8).

Figure 7: Parameter estimates from wind damage model. Points show the median coefficient estimates from the 200 bootstrapped model fits, whiskers show bootstrapped 95% confidence interval.

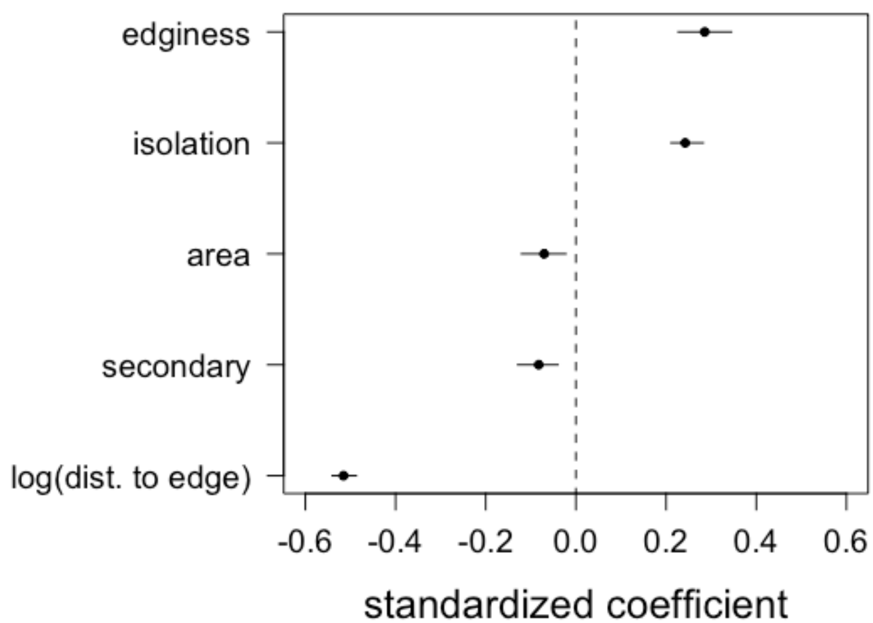

Figure 8: Model predictions of ΔNPV and the fragmentation predictors. Solid lines depict predictions of the median coefficient estimates from bootstrapped model fits, dashed lines and shaded areas show predictions of 2.5 and 97.5% quantiles of coefficient estimates. a) distance from edge. b) patch area. c) edginess. d) isolation.

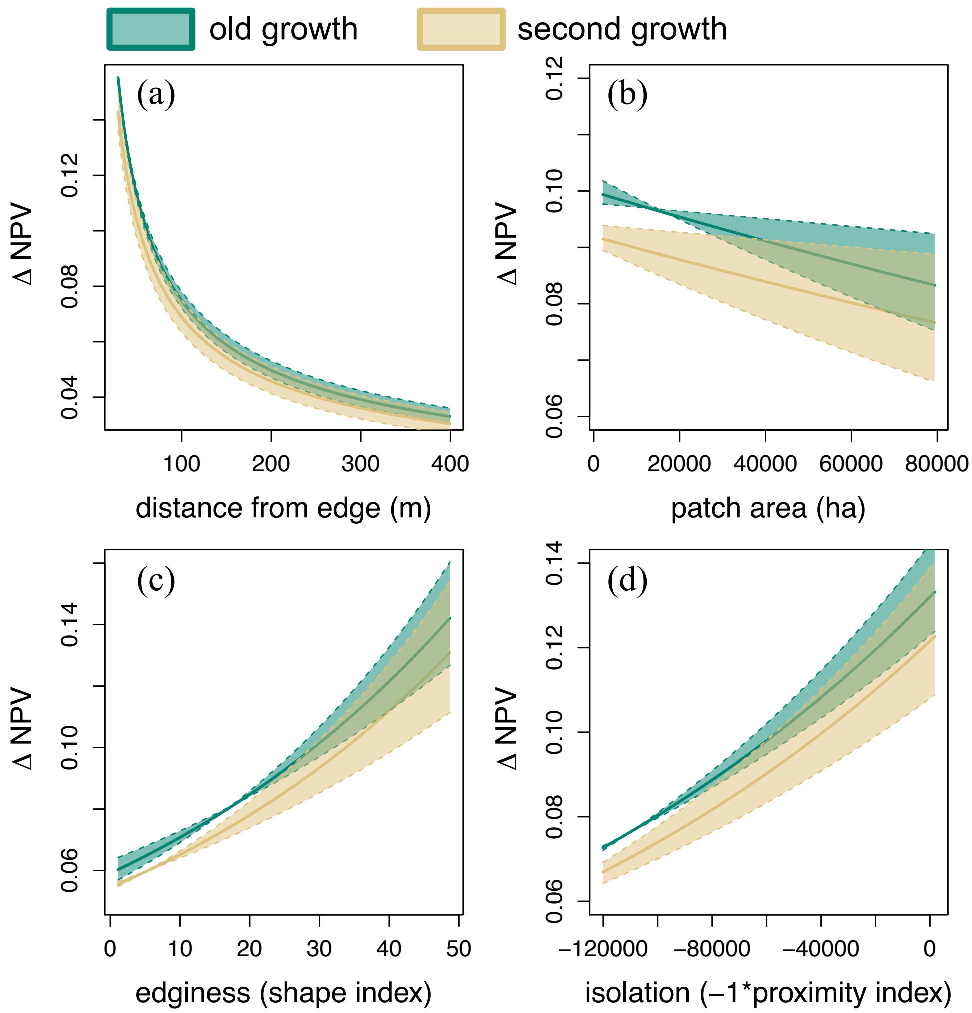

Discussion

Effects of fragmentation on wind damage

This study provides the first strong empirical evidence that fragmentation increases risk of damage from extreme wind events in tropical forests. The severe convection event that occurred in our study region caused an overall loss on the order of 1.7 x 10^{-3} Pg C in the study area. When averaged across the total forested area in the study area (95,596 ha), this amounts to ~17.8 Mg C ha^{-1}, more than six times greater per hectare than figures from a recent study that estimated annual carbon loss from natural disturbances in the entire Amazon forest (Espírito-Santo et al., 2014). That study estimated the total loss at 1.88 Pg C y^{-1}, an average of 2.8 Mg C ha^{-1} across the ~6.8 x 10^8 ha of Amazon forest.

A number of differences between their study and ours could explain the discrepancy. The Espírito-Santo et al. study mapped disturbances across a study area many times the size of ours, and developed a disturbance size-frequency distribution for the entire Amazon. The disturbances captured in our far smaller study are likely on the intermediate-to-large end of their disturbance size-frequency distribution. However, the discrepancy might also be due to differences in landscape structure in the two studies. Espírito-Santo et al. focused on contiguous forest, where, based on our results, wind damage is likely to be less severe than in the fragmented landscapes of our study region. These findings illustrate the importance of considering fragmented landscapes when assessing disturbance regimes in tropical forests. Studies that do not consider the effects of landscape configuration may underestimate the importance of wind disturbance for quantifying tropical forest carbon sinks, especially given that recent estimates suggest 70% of the world's forests are within 1 km of a forest edge (Haddad et al., 2015),

Though many studies suggest that fragmented forests should have heightened vulnerability to wind damage (Saunders *et al.*, 1991; Laurance & Curran, 2008), evidence for this phenomenon has been lacking. For example, a number of studies that set out to measure effects of fragmentation on wind damage after Cyclone Larry, a category 5 tropical cyclone, found little difference in wind damage between fragments and continuous forest (Catterall *et al.*, 2008; Grimbacher *et al.*, 2008; Pohlman *et al.*, 2008).

Our study may have detected an effect where former studies did not for several reasons. First, the storm we considered was not as intense as a Cyclone Larry, and continuous forest cover may provide a protective benefit only up to a certain degree of storm intensity (Catterall et al. 2008). We do not have precise wind speed measurements from the date of the storm, but the presence and intensity of overshooting tops indicates that winds were probably ≥ 93 km/h (Bedka and Khlopenkov, 2016). In contrast, Category 5 tropical storms are associated with sustained winds > 200 km/h. Lending support to this hypothesis, a study after Hurricane Hugo in South Carolina found that in areas struck by the most intense part of the hurricane, species differences in wind resistance were not apparent (Hook *et al.*, 1991). Differences in rates of damage across species were only observed in areas where wind speeds were lower. Variation in exposure and vulnerability to extreme winds due to species composition and landscape configuration may come into play only when winds are not so severe that they cause widespread damage regardless.

Second, previous studies of fragmentation and wind damage were based on field data from a relatively small number of plots. Heterogeneity in damage and wind speeds may have affected the statistical ability to detect underlying patterns related to fragmentation (Grimbacher *et al.*, 2008). This patchiness and unmodeled variation in wind speeds is likely the reason for the substantial unexplained variance in our statistical models. However, because our remote sensing approach allows us to consider a broad landscape with a large sample size we are able to detect an effect of fragmentation despite the noise, demonstrating, as many other studies have, the usefulness of remote sensing for understanding ecosystems at landscape-to-regional scales (Chambers et al. 2007).

Fragmented forests may be more prone to wind damage via two main mechanisms: because they are exposed to stronger winds than continuous forest, or because they are more vulnerable to strong winds due to differences in species composition or forest structure (Laurance and Curran 2008). We found effects of all three axes of fragmentation – isolation, edge, and area – on wind damage, which suggest possible support for both mechanisms. The effects of isolation are probably due to exposure to stronger winds. Forest slows wind down; rougher surfaces exert more drag leading to slower wind speeds (Davies-Colley *et al.*, 2000). Wind picks up more speed over smoother vegetation types, like pasture. Because our measure of isolation only takes into account the landscape surrounding a patch, and no characteristics of the patch itself, our finding that wind damage was more severe in more isolated fragments probably reflects exposure to stronger wind speeds in isolated patches, rather than differences in species composition or structure across patches.

Edge and area effects on wind damage are more difficult to attribute to exposure versus vulnerability, and could be due to either or both mechanisms. We found that pixels close to forest edges and pixels in edgier patches were more likely to be severely damaged. We also found a weak effect of patch size, likely because pixels in smaller patches are closer to edges. Forest edges are exposed to stronger winds (Somerville, 1980; Morse *et al.*, 2002), but there are also well-documented edge effects on species composition that could increase vulnerability to wind damage (Oosterhoorn & Kappelle, 2000; Laurance *et al.*, 2006). The degree to which differences in exposure or vulnerability explain the relationship between fragmentation and wind damage has implications for management actions to minimize impacts of strong winds. Future research could focus on disentangling the mechanisms responsible for these patterns.

Wind damage in old- vs. second-growth forest

When controlling for fragmentation, second-growth forests suffer slightly lower damage than old-growth forests, counter to our initial hypothesis. Because trees with lower wood density are more prone to wind damage and community mean wood density tends to increase over succession in wet tropical forests (Bazzaz & Pickett, 1980; Lohbeck *et al.*, 2013), we hypothesized that wind damage would be more severe in second-growth forests. Our finding to the contrary may be due to differences in tree stature between old-growth and second-growth forests. Larger trees are more susceptible to wind damage, in particular to uprooting (Putz *et al.*, 1983; Zimmerman *et al.*, 1994; Everham & Brokaw, 1996; Canham *et al.*, 2010), which translates into differences in damage across sites with different forest structure. For example, Uriarte et al. (2004) found that damage after Hurricane Georges in the Dominican Republic was higher in sites with higher basal area and that young forests with low basal area were not severely affected by hurricane. Similarly, McGroddy et al. (2013) found that forest stands in the southern Yucatan with taller canopies and higher basal area suffered more severe hurricane damage, and that these structural differences were associated with past land use.

We further suspect that these differences are due to forest structure, and not species composition, because the way we distinguished between old-growth and second-growth forests in our land cover map does not detect differences in species composition.

Rather, the difference between old-growth and second-growth forest is determined by spectral properties that relate to stand structure (Gutiérrez-Vélez *et al.*, 2011). Furthermore, because of the high levels of anthropogenic disturbance in the study area, we do not necessarily expect the successional shifts in species composition that are predicted for relatively undisturbed forests. Old-growth forests in the study area have never been completely cleared, but they have still been subject to anthropogenic disturbance, such as selective logging. Selective logging tends to target timber species with higher wood density (Verburg & van Eijk-Bos, 2003), so the largest remaining trees in selectively logged forests may be soft-wooded species. Large stature and soft wood would make these stands especially prone to wind damage, perhaps explaining the higher damage we observed in old-growth forests.

In our model, however, fragmentation had a much stronger influence on damage than forest type (Figure 7, 9). Second-growth forests in the study area are more fragmented than old-growth forests, which ultimately might result in more severe wind impacts in these forests. Elsewhere, studies have found that second growth tends to happen along forest margins and in small fragments surrounded by non-forest land use (Helmer, 2000; Asner *et al.*, 2009; Sloan *et al.*, 2015). Wind is not the only disturbance for which risk is higher along edges: fire in the Amazon tends to be concentrated along forest edges (Cochrane & Laurance, 2002; Alencar *et al.*, 2004; Armenteras *et al.*, 2013). There is potential for wind and fire to interact and amplify the other's impacts: studies in temperate ecosystems have found that an earlier fire can increase the severity of subsequent blow downs, and wind damage can increase the risk of fire by adding fuels and opening up the forest canopy (Myers & van Lear, 1998; Kulakowski & Veblen, 2002; Kulakowski & Veblen, 2007). These interactions might occur in the Amazon, and could exacerbate disturbance effects on forest carbon balance.

Wind and other disturbances can alter successional pathways in regrowing forests (Anderson-Teixeira *et al.*, 2013; Uriarte et al 2016). Variability in disturbance risk should thus be taken into account in spatial planning, management, and carbon accounting in tropical second-growth forests where the goal is to promote carbon sequestration. Silviculture has long considered wind damage risk in site and species selection and planting configuration (Somerville, 1980; Savill, 1983; Talkkari *et al.*, 2000). However, managing tropical second-growth forests for carbon is a relatively new endeavor and the way landscape configuration influences susceptibility to disturbance is not well understood for tropical forests (US DOE, 2012). However, where possible, and where risk of extreme winds is high, minimizing fragmentation and isolation could reduce risk of wind damage.

Future research should attempt to disentangle the mechanisms behind the patterns observed in this study. Understanding the degree to which differences in vulnerability versus exposure underlie variation in wind impacts will clarify appropriate management actions to minimize risk of wind damage in second-growth or remnant forests. Fragmentation experiments such as the Biological Dynamics of Forest Fragments experiment in Brazil have shed light on how fragmentation affects forest composition, structure, and microclimate (Laurance *et al.*, 2002). However, understanding what those changes mean for impacts of extreme winds is not straightforward, and doing so would require some “luck” in that a severe windstorm would have to strike the experiment. This limitation presents some challenges in studying mechanisms of wind damage in fragmented landscapes, but there are ways forward. Fragmentation experiments like the aforementioned, but located in landscapes that suffer frequent severe wind events, such as Caribbean forests, could be useful in that the likelihood of extreme winds striking an experiment would be higher. However, an experimental approach relying on random chance is not the only way to further investigate these mechanisms. Improvements in modeling and mapping wind speed and in our understanding of how wind interacts with complex landscapes will further shed light on how exposure varies with fragmentation. Advances in remote sensing technology, which are beginning to provide a more detailed picture of forest structure and composition, will be useful in understanding ecological mechanisms responsible for variability in disturbance impacts (Chambers *et al.*, 2007). Finally, much of what we already know about variation in species and stand susceptibility to wind comes from opportunistic field sampling after extreme winds (e.g. Zimmerman *et al.*, 1994; Uriarte *et al.*, 2004; McGroddy *et al.*, 2013), and there is a need for further opportunistic post-storm sampling in fragmented landscapes. Continued monitoring of forest disturbance in fragmented landscapes, such as with the remote sensing approach demonstrated in this paper, is essential so that such opportunities are not lost. An improved understanding of how and why fragmentation and landscape configuration influence disturbance regimes in tropical second-growth forests will help ensure that the carbon potential of tropical second-growth forests is maximally achieved.

Acknowledgements

We thank C. Gabriel Hidalgo, Luís Calderon Vasquez, Robert Piña, and Geancarlo Cohello for assistance with fieldwork. Thanks to the Uriarte and DeFries lab groups, and

Bianca Lopez, for helpful feedback on early drafts of this manuscript. We acknowledge support from the Institute for Latin American Studies at Columbia University, and the Center for International Forestry Research (CIFOR).

References

Adams JB, Gillespie AR (2006) *Remote Sensing of Landscapes with Spectral Images*. Cambridge, UK: Cambridge University Press.

Alencar AAC, Solorzano LA, Nepstad DC (2004) Modeling forest understory fires in an eastern Amazonian landscape. Ecological Applications, **14**, 139–149.

Anderson-Teixeira KJ, Miller AD, Mohan JE, Hudiburg TW, Duval BD, DeLucia EH (2013) Altered dynamics of forest recovery under a changing climate. Global Change Biology, **19**, 2001–2021.

Armenteras D, González TM, Retana J (2013) Forest fragmentation and edge influence on fire occurrence and intensity under different management types in Amazon forests. Biological Conservation, **159**, 73–79.

Asner GP, Rudel TK, Aide TM, DeFries R, Emerson R (2009) A Contemporary Assessment of Change in Humid Tropical Forests. Conservation Biology, **23**, 1386–1395.

Bazzaz FA, Pickett S (1980) Physiological ecology of tropical succession: a comparative review. Annual review of ecology and systematics, **11**, 287–310.

Bedka, KM, Khlopenkov K (2016) A probabilistic multispectral pattern recognition method for detection of overshooting cloud tops using passive satellite imager observations. Journal of Applied Meteorology And Climatology. In press.

Bellingham PJ, Kapos V, Varty N (1992) Hurricanes need not cause high mortality: the effects of Hurricane Gilbert on forests in Jamaica. Journal of Tropical Ecology, **8**, 217-223.

Boardman JW, Kruse FA, Green RO (1995) Mapping target signatures via partial unmixing of AVIRIS data. *Proceedings of the Fifth JPL Airborne Earth Science Workshop. JPL Publication, vol. 95-01 (pp. 23 – 26).* Pasadena, CA: Jet Propul. Lab.

Breiman L (2001) Random Forests. Machine Learning, **45**, 5–32.

Brown S, Lugo AE (1982) The storage and production of organic matter in tropical forests and their role in the global carbon cycle. Biotropica **14**, 161–187

Canham CD, Thompson J, Zimmerman JK, Uriarte M (2010) Variation in Susceptibility to Hurricane Damage as a Function of Storm Intensity in Puerto Rican Tree Species. Biotropica, **42**, 87–94.

Canham CD, Papaik MJ, Latty EF (2001) Interspecific variation in susceptibility to windthrow as a function of tree size and storm severity for northern temperate tree species. Canadian Journal of Forest Research, **31**, 1–10.

Canty MJ, Nielsen AA (2008) Automatic radiometric normalization of multitemporal satellite imagery with the iteratively re-weighted MAD transformation. Remote Sensing of Environment, **112**, 1025–1036.

Catterall CP, McKenna S, Kanowski J, Piper SD (2008) Do cyclones and forest fragmentation have synergistic effects? A before–after study of rainforest vegetation structure at multiple sites. Austral Ecology, **33**, 471–484.

Chambers JQ, Asner GP, Morton DC et al. (2007) Regional ecosystem structure and function: ecological insights from remote sensing of tropical forests. Trends in Ecology & Evolution, **22**, 414–423.

Chambers JQ, Negrón-Juárez RI, Hurtt GC, Marra DM, Higuchi N (2009) Lack of intermediate-scale disturbance data prevents robust extrapolation of plot-level tree mortality rates for old-growth tropical forests. Ecology Letters, **12**, E22–E25.

Chambers JQ, Negrón-Juárez RI, Marra DM et al. (2013) The steady-state mosaic of disturbance and succession across an old-growth Central Amazon forest landscape. Proceedings of the National Academy of Sciences, **110**, 3949–3954.

Cochrane MA, Laurance WF (2002) Fire as a large-scale edge effect in Amazonian forests. *Journal of Tropical Ecology*, **18**, 311–325.

Curran TJ, Brown RL, Edwards E *et al.* (2008) Plant functional traits explain interspecific differences in immediate cyclone damage to trees of an endangered rainforest community in north Queensland. Austral Ecology, **33**, 451–461.

D'Angelo SA, Andrade ACS, Laurance SG, Laurance WF, Mesquita RCG (2004) Inferred causes of tree mortality in fragmented and intact Amazonian forests. Journal of Tropical Ecology, **20**, 243–246.

Davies-Colley RJ, Payne GW, Van Elswijk M (2000) Microclimate gradients across a forest edge. New Zealand Journal of Ecology, **24**, 111-121.

de Casaneve JL, Pelotto JP, Protomastro J (1995) Edge-Interior Differences in Vegetation Structure and Composition in a Chaco Semiarid Forest, Argentina. Forest Ecology and Management, **72**, 61–69.

Del Genio AD, Yao M-S, Jonas J (2007) Will moist convection be stronger in a warmer climate? *Geophysical Research Letters*, **34**, L16703.

Di Vittorio AV, Negrón-Juárez RI, Higuchi N, Chambers JQ (2014) Tropical forest carbon balance: effects of field- and satellite-based mortality regimes on the dynamics and the spatial structure of Central Amazon forest biomass. Environmental Research Letters, **9**, 034010.

Dormann CF, Elith J, Bacher S et al. (2012) Collinearity: a review of methods to deal with it and a simulation study evaluating their performance. Ecography, **36**, 27–46.

Dworak, R., K. M. Bedka, J. Brunner, and W. Feltz, 2012: Comparison between GOES-12 overshooting top detections, WSR-88D radar reflectivity, and severe storm reports. Weather and Forecasting, **10**, 1811-1822.

Espírito-Santo FDB, Keller M, Braswell B, Nelson BW, Frolking S, Vicente G (2010) Storm intensity and old-growth forest disturbances in the Amazon region. Geophysical Research Letters, **37**, L11403.

Espírito-Santo FDB, Keller MM, Linder E, Oliveira Junior RC, Pereira C, Oliveira CG (2014) Gap formation and carbon cycling in the Brazilian Amazon: measurement using high-resolution optical remote sensing and studies in large forest plots. Plant Ecology & Diversity, **7**, 305–318.

Everham EM, Brokaw NV (1996) Forest damage and recovery from catastrophic wind. The botanical review, **62**, 113–185.

Fahrig L (2003) Effects of habitat fragmentation on biodiversity. Annual Review of

Ecology, Evolution, and Systematics, **34**, 487–515.
Ferreira LV, Laurance WF (1997) Effects of forest fragmentation on mortality and damage of selected trees in central Amazonia. Conservation Biology, **11**, 797–801.
Fisher JI, Hurtt GC, Thomas RQ, Chambers JQ (2008) Clustered disturbances lead to bias in large-scale estimates based on forest sample plots. Ecology Letters, **11**, 554–563.
Flynn DFB, Uriarte M, Crk T, Pascarella JB, Zimmerman JK, Aide TM, Caraballo Ortiz MA (2009) Hurricane Disturbance Alters Secondary Forest Recovery in Puerto Rico. Biotropica, **42**, 149–157.
Fons WL (1940) Influence of forest cover on wind velocity. Journal of Forestry, **38**, 481-486.
Fox J, Monette G (1992) Generalized Collinearity Diagnostics. Journal of the American Statistical Association, **87**, 178–183.
Garstang M, Massie HL, Halverson J, Greco S, Scala J (1994) Amazon Coastal Squall Lines.1. Structure and Kinematics. Monthly Weather Review, **122**, 608–622.
Garstang M, White S, Shugart HH, Halverson J (1998) Convective cloud downdrafts as the cause of large blowdowns in the Amazon rainforest. Meteorology and Atmospheric Physics, **67**, 199–212.
Grimbacher PS, Catterall CP, Stork NE (2008) Do edge effects increase the susceptibility of rainforest fragments to structural damage resulting from a severe tropical cyclone? Austral Ecology, **33**, 525–531.
Grove SJ, Turton SM, Siegenthaler DT (2000) Mosaics of canopy openness induced by tropical cyclones in lowland rain forests with contrasting management histories in northeastern Australia. Journal of Tropical Ecology, **16**, 883–894.
Gutiérrez-Vélez VH, DeFries R (2013) Annual multi-resolution detection of land cover conversion to oil palm in the Peruvian Amazon. Remote Sensing of Environment, **129**, 154–167.
Gutiérrez-Vélez VH, DeFries R, Pinedo-Vasquez M et al. (2011) High-yield oil palm expansion spares land at the expense of forests in the Peruvian Amazon. Environmental Research Letters, **6**, 044029.
Haddad NM, Brudvig LA, Clobert J et al. (2015) Habitat fragmentation and its lasting impact on Earth's ecosystems. Science Advances, **1**, e1500052–e1500052.
Haralick RM, Shanmugam K (1973) Textural features for image classification. IEEE Transactions on Systems, Man, and Cybernetics. **33**, 610-621.
Harper KA, Macdonald SE, Burton PJ et al. (2005) Edge influence on forest structure and composition in fragmented landscapes. Conservation Biology, **19**, 768–782.
Helmer EH (2000) The Landscape Ecology of Tropical Secondary Forest in Montane Costa Rica. Ecosystems, **3**, 98–114.
Hook DD, Buford MA, Williams TM (1991) Impact of Hurricane Hugo on the South Carolina coastal plain forest. Journal of Coastal Research, **8**, 291-300.
Imbert D, Labbe P, Rousteau A (1996) Hurricane damage and forest structure in Guadeloupe, French West Indies. Journal of Tropical Ecology, **12**, 663-680.
Kanowski J, Catterall CP, McKenna SG, Jensen R (2008) Impacts of cyclone Larry on the vegetation structure of timber plantations, restoration plantings and rainforest on the Atherton Tableland, Australia. Austral Ecology, **33**, 485–494.
Knutson TR, McBbride JL, Chan J et al. (2010) Tropical cyclones and climate change.

Nature Geoscience, **3**, 157–163.

Kulakowski D, Veblen TT (2002) Influences of fire history and topography on the pattern of a severe wind blowdown in a Colorado subalpine forest. Journal of Ecology, **90,** 806-819.

Kulakowski D, Veblen TT (2007) Effect of prior disturbances on the extent and severity of wildfire in Colorado subalpine forests. Ecology, **88**, 759–769.

Laurance WF (2004) Forest-climate interactions in fragmented tropical landscapes. Philosophical Transactions of the Royal Society B: Biological Sciences, **359**, 345–352.

Laurance WF, Curran TJ (2008) Impacts of wind disturbance on fragmented tropical forests: A review and synthesis. Austral Ecology, **33**, 399–408.

Laurance WF, Ferreira LV, Rankin-de Merona JM, Laurance SG (1998) Rain forest fragmentation and the dynamics of Amazonian tree communities. Ecology, **79**, 2032–2040.

Laurance WF, Laurance SG, Ferreira LV, Rankin-de Merona JM, Gascon C, Lovejoy TE (1997a) Biomass collapse in Amazonian forest fragments. Science, **278**, 1117–1118.

Laurance WF, Laurance SG, Ferreira LV, RankindeMerona JM, Gascon C, Lovejoy TE (1997b) Biomass collapse in Amazonian forest fragments. Science, **278**, 1117–1118.

Laurance WF, Lovejoy TE, Vasconcelos HL et al. (2002) Ecosystem decay of Amazonian forest fragments: A 22-year investigation. Conservation Biology, **16**, 605–618.

Laurance WF, Nascimento HEM, Laurance SG, Andrade AC, Fearnside PM, Ribeiro JEL, Capretz RL (2006) Rain forest fragmentation and the proliferation of successional trees. Ecology, **87**, 469–482.

Locatelli B, Catterall CP, Imbach P, Kumar C (2015) Tropical reforestation and climate change: beyond carbon. Restoration Ecology, **23,** 337-343

Loehle C (1991) Managing and monitoring ecosystems in the face of heterogeneity. In: *Ecological heterogeneity* (eds Kolasa J, Pickett STA). Springer Verlag, New York, NY.

Lohbeck M, Poorter L, Lebrija-Trejos E et al. (2013) Successional changes in functional composition contrast for dry and wet tropical forest. Ecology, **94**, 1211–1216.

Lugo AE (2008) Visible and invisible effects of hurricanes on forest ecosystems: an international review. Austral Ecology, **33**, 368–398.

McGroddy M, Lawrence D, Schneider L, Rogan J, Zager I, Schmook B (2013) Forest Ecology and Management. Forest Ecology and Management, **310**, 812–820.

Mesquita R, Delamônica P, Laurance WF (1999) Effect of surrounding vegetation on edge-related tree mortality in Amazonian forest fragments. Biological Conservation, **91,** 129-134.

Morse AP, Gardiner BA, Marshall BJ (2002) Mechanisms controlling turbulence development across a forest edge. Boundary-Layer Meteorology, **103**, 227–251.

Myers RK, van Lear DH (1998) Hurricane-fire interactions in coastal forests of the south: a review and hypothesis. Forest Ecology and Management, **103**, 265–276.

Negrón-Juárez RI, Chambers JQ, Guimaraes G et al. (2010) Widespread Amazon forest tree mortality from a single cross-basin squall line event. Geophysical Research Letters, **37**, L16701.

Negrón-Juárez RI, Chambers JQ, Marra DM, Ribeiro GHPM, Rifai SW, Higuchi N,

Roberts D (2011) Remote Sensing of Environment. Remote Sensing of Environment, **115**, 3322–3328.
Nelson BW, Kapos V, Adams JB, Oliveira WJ, Braun OP (1994) Forest disturbance by large blowdowns in the Brazilian Amazon. Ecology, **75**, 853–858.
Oliveira PJC, Asner GP, Knapp DE et al. (2007) Land-use allocation protects the Peruvian Amazon. Science, **317**, 1233–1236.
Oliver HR (1971) Wind profiles in and above a forest canopy. Quarterly Journal of the Royal Meteorological Society, **97,** 548-553.
Oosterhoorn M, Kappelle M (2000) Vegetation structure and composition along an interior-edge-exterior gradient in a Costa Rican montane cloud forest. Forest Ecology and Management, **126**, 291–307.
Orlowsky B, Seneviratne SI (2012) Global changes in extreme events: regional and seasonal dimension. Climatic Change, **110,** 669-696.
Peltola H (1996) Model computations on wind flow and turning moment by wind for Scots pines along the margins of clear-cut areas. Forest Ecology and Management, **83,** 203-215.
Pohlman CL, Goosem M, Turton SM (2008) Effects of Severe Tropical Cyclone Larry on rainforest vegetation and understorey microclimate near a road, powerline and stream. Austral Ecology, **33**, 503–515.
Poorter L, Bongers F, Aide TM et al. (2016) Biomass resilience of Neotropical secondary forests. Nature, **530**, 211–214.
Putz FE, Coley PD, Lu K, Montalvo A, Aiello A (1983) Uprooting and snapping of trees: structural determinants and ecological consequences. Canadian Journal of Forest Research, **13**, 1011–1020.
Ramos da Silva R, Werth D, Avissar R (2008) Regional Impacts of Future Land-Cover Changes on the Amazon Basin Wet-Season Climate. Journal of Climate, **21**, 1153–1170.
Rifai SW, Urquiza Muñoz JD, Negrón-Juárez RI, *et al.* (2016) Landscape-scale consequences of differential tree mortality from catastrophic wind disturbance in the Amazon. Ecological Applications, in press.
Roberts DA, Numata I, Holmes K, et al. (2002) Large area mapping of land-cover change in Rondônia using multitemporal spectral mixture analysis and decision tree classifiers. Journal of Geophysical Research, **107**, 8073.
Rodriguez-Galiano VF, Chica-Olmo M, Abarca-Hernandez F, Atkinson PM, Jeganathan C (2012) Remote Sensing of Environment. Remote Sensing of Environment, **121**, 93–107.
Saunders DA, Hobbs RJ, Margules CR (1991) Biological Consequences of Ecosystem Fragmentation - a Review. Conservation Biology, **5**, 18–32.
Savill PS (1983) Silviculture in windy climates. Forestry Abstracts, **44,** 473-488.
Sloan S, Goosem M, Laurance SG (2015) Tropical forest regeneration following land abandonment is driven by primary rainforest distribution in an old pastoral region. Landscape Ecology, **31**, 601–618.
Somerville A (1980) Wind Stability - Forest Layout and Silviculture. New Zealand Journal of Forestry Science, **10**, 476–501.
Talkkari A, Peltola H, Kellomäki S, Strandman H (2000) Integration of component models from the tree, stand and regional levels to assess the risk of wind damage at

forest margins. Forest Ecology and Management **135,** 303-313.

Uriarte M, Rivera LW, Zimmerman JK, Aide TM, Power AG, Flecker AS (2004) Effects of land use history on hurricane damage and recovery in a neotropical forest. Plant Ecology, **174,** 49-58.

Uriarte M, Clark JS, Zimmerman JK, Comita LS, Forero-Montaña J, Thompson J (2012) Multidimensional trade-offs in species responses to disturbance: implications for diversity in a subtropical forest. Ecology, **93**, 191–205.

Uriarte, M., N.B. Schwartz, Powers, J.S., Marin-Spiotta, E., Liao, W., and Werden, L. in revision. Impacts of climate variability on tree demography in tropical second-growth forests: The importance of regional context for predicting successional trajectories. Biotropica.

US DOE (2012) *Research Priorities for Tropical Ecosystems Under Climate Change Workshop Report*. U.S. Department of Energy Office of Science, 134 p.

Verburg R, van Eijk-Bos C (2003) Effects of selective logging on tree diversity, composition and plant functional type patterns in a Bornean rain forest. Journal of Vegetation Science, **14**, 99–110.

Zeng H, Peltola H, Talkkari A, Venäläinen A, Strandman H, Kellomäki S, Wang K (2004) Influence of clear-cutting on the risk of wind damage at forest edges. Forest Ecology and Management, **203**, 77–88.

Zhu Z, Woodcock CE (2012) Remote Sensing of Environment. Remote Sensing of Environment, **118**, 83–94.

Zimmerman JK, Everham EM III, Waide RB, Lodge DJ, Taylor CM, Brokaw NV (1994) Responses of tree species to hurricane winds in subtropical wet forest in Puerto Rico: implications for tropical tree life histories. The Journal of Ecology, 911–922.